

# Study on the Mineral Materials' Adsorption Properties of Radioactive Chemical Elements

Keke Chen

College of Chemistry and Chemical Engineering, Xinxiang University, Xinxiang 453003, China  
[lisa820928@126.com](mailto:lisa820928@126.com)

This paper studies the mineral materials' adsorption properties of radioactive chemical elements, it takes the adsorption behavior of uranium (VI) by the synthetic ternary Ca-Mg-Al hydrotalcite as an example, starts from designing and assembling the highly acid-resistant hydrotalcite materials which contain various functional groups, successfully prepares three kinds of hydrotalcite materials by two basic processing technologies, then by using SEM, FT-IR, XPS and other surface technologies and conducting many adsorption experiments, this paper explores and studies the action mechanism and interface effect of the hydrotalcite materials' adsorption of U(VI). Finally, it obtains relevant conclusions: a series of synthetic LDHs functional materials can be applied to the separation and concentration of radionuclides, and it is further confirmed that, during the U(VI) adsorption process, Ca-Mg-Al-LDH and Ca-Mg-Al-LDOx have surface complexation and electrostatic interaction, and the research results are of great significance for the development and use of efficient, cheap, and sustainable adsorbent materials in the future.

## 1. Introduction

Hydrotalcite clay minerals, which are popular in the market today, are well-known for their advantages of better "memory effect" and exchangeable interlayer anions, and have been widely used in many fields such as energy storage, environmental remediation, and nano-catalysis, especially in the field of environmental remediation, due to their excellent performance of natural, clean and low-price, they have been widely used (Anirudhan and Jalajamony 2013).

In the past five years, the study on the adsorption of uranyl ions by pure hydrotalcite materials has just begun. The relevant adsorption mechanism and theoretical research content still need to be enriched continuously, and hydrotalcite is prone to poor acid resistance and low saturated adsorption capacity (Anirudhan and Jalajamony, 2013). Therefore, through the high-temperature calcination method and the hydrothermal polymerization method, combined with the advantages of inter-layer ions of hydrotalcite, its combination with other elements to form new chemical properties can play a role in controlling the chemical structure, finally, the purpose of increasing the number of oxygen-containing groups on the surface and between the layers can be achieved, and the hydrophilicity is also enhanced, so that the problems of low uranyl ion adsorption capacity and poor acid resistance of hydrotalcite can be solved, and a hydrotalcite structural system with controllable multi-morphology and multi-functionality can be formed (Durán-Blanco et al., 2013).

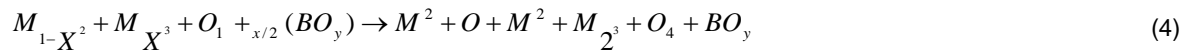
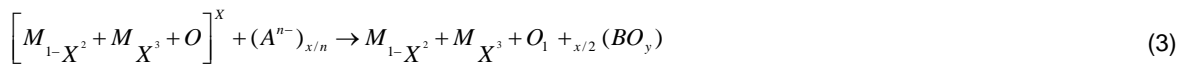
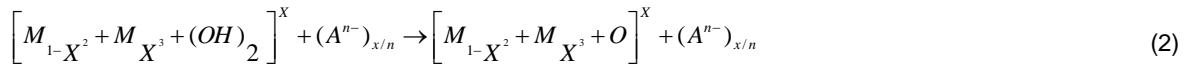
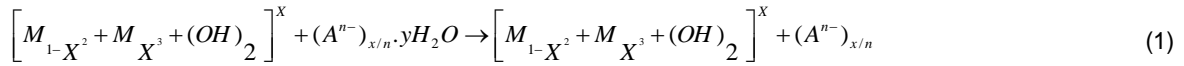
This paper focuses on the use of FT-IR, XRD, XPS and SEM technologies to study the micro-morphology and structural characteristics of hydrotalcite materials, and then analyze the problems of different environments in the adsorption process. The research of this paper has an important role in finding the mechanism of interaction between hydrotalcite and uranyl ions, analyzing the migration mechanism and behavioral characteristics of uranyl ions in special environments is of great scientific and practical value significance.

## 2. Hydrotalcite adsorption behavior of uranium

### 2.1 Application environment analysis of hydrotalcite

The ternary hydrotalcite material we often refer to is a composite material with similar crystal structure formed by mixing three kinds of bivalent or trivalent metal elements (Cheng et al., 2018). The high-temperature

calcination method used in the study is a highly efficient technique by which the surface defects of the derivative product can be improved and the inner layer reaction is favored (Li et al., 2013). Hydrotalcite after calcination, also known as Layered Double Hydroxide (LDH), has a good "memory effect" (Li et al., 2013). The calcination process of hydrotalcite is divided into four different processes: dehydration process, dehydroxylation process, interlayer anion decomposition and oxidation recombination process (Suc, 2012). The theoretical formula of calcination process is shown as Formula 1:



When the calcination temperature  $T < 600^\circ\text{C}$ , the material will have a certain "memory effect", and when  $T > 600^\circ\text{C}$ , the "memory effect" of the material will be destroyed, during the calcination process, the material gradually changes into LDH material. In many cases, it can exhibit better adsorption properties.

In this paper, three elements Ca, Mg and Al are selected as the metal source, hydrothermal synthesis technology is used to synthesize hydrotalcite material under alkaline conditions, at last, with the help of high-temperature calcination technology, at  $200^\circ\text{C}$ ,  $300^\circ\text{C}$ ,  $400^\circ\text{C}$ ,  $500^\circ\text{C}$  and  $600^\circ\text{C}$  temperature conditions, hydrotalcite materials and additional derivatives are synthesized, and the controllability of the adsorption properties of various materials at different temperatures is compared.

## 2.2 Experimental reagents and instruments

Sodium nitrate, sodium carbonate, uranyl nitrate, calcium nitrate tetrahydrate, aluminum nitrate nonahydrate, urea, sodium hydroxide, and magnesium nitrate hexahydrate, all reagents are analytical reagents (AR) (Hennig et al., 2012). IS126 standard pH meter, UV-2550 UV spectrophotometer, JSM-6330F scanning electron microscope, ASAP2020 specific surface area tester, Nicolet Magana-IR750 Fourier transform infrared spectrometer, X-ray diffractometer and other equipment (Molera and Eriksen, 2002).

## 2.3 Preparation of adsorbents

The basic production process of the calcined hydrotalcite material can be expressed as follows: Take 0.6g of Ca-Mg-Al-LDH raw material, ensure it is fully dried, grind into powder, place the powder in a crucible and calcine in a muffle furnace at high temperature ( $x^\circ\text{C}$ ) for 3 hours. After the reaction is completed, take out the powder and wash it several times with deionized water and absolute ethanol, at last, dry it at  $10^\circ\text{C}$  in the vacuum, then the Ca-Mg-Al-LDO $x$  ( $x$ :  $200^\circ\text{C}$ .,  $300^\circ\text{C}$ .,  $400^\circ\text{C}$ .,  $500^\circ\text{C}$  and  $600^\circ\text{C}$ ) is obtained (Bonhoure et al., 2002). The synthesis route of the material can be represented as shown in Figure 1.

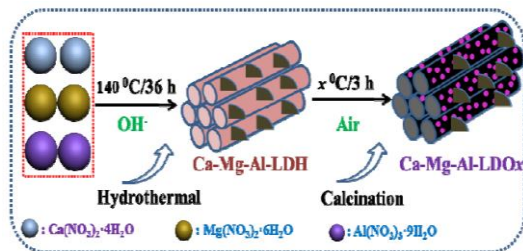


Figure 1: Proposed hydrothermal synthesis and calcination route of Ca-Mg-Al-LDH and Ca-Mg-Al-LDO $x$

## 3. Analysis process and discussion

### 3.1 Characterization analysis

The basic form and micro-morphology of Ca-Mg-Al-LDH, Ca-Mg-Al-LDO300 and Ca-Mg-Al-LDO600 samples prepared by calcination are determined by scanning electron microscopy (SEM) (Nakata et al., 2002), the

results are shown as Figure 2. From the analysis of the figure, it can be seen that the morphology of the three samples all shows the characteristics of rod-like structures, and the ordered and regular structures are more obvious.

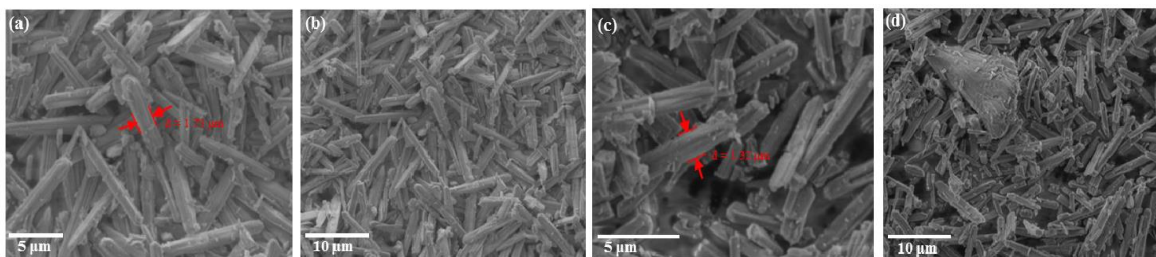


Figure 2: Ca-Mg-Al-LDH(a)&(b), Ca-Mg-Al-LDO300(c)&(d) and Ca-Mg-Al-LDO 600 (e)&(f) ((e) and (f))

EDS and element mapping are used to carry out content chemical analysis of the prepared samples respectively. The content distribution of elements corresponding to the test results is shown as Table 1. The test results in the analysis table show that: Ca, Mg, Al, and O constitute the main components of the sample. As the calcination temperature progressively increases, the content of Ca in the sample continuously increases. When the calcination temperature reaches 600°C, the Ca content reaches 1.27%.

Table 1: Relative elemental distribution percentages of EDS analysis for Ca-Mg-Al-LDH(a)&(b), Ca-Mg-Al-LDO 300°C&(d) and Ca-Mg-Al-LDO 600°C

Atomic ratio%	Ca	Mg	Al	O
Ca-Mg-Al-LDH	0.27%	60.5%	13.82%	25.32%
Ca-Mg-Al-LDO300	0.7%	10.9%	23.81%	64.59%
Ca-Mg-Al-LDO 600	1.27%	5.14%	34.77%	58.86%

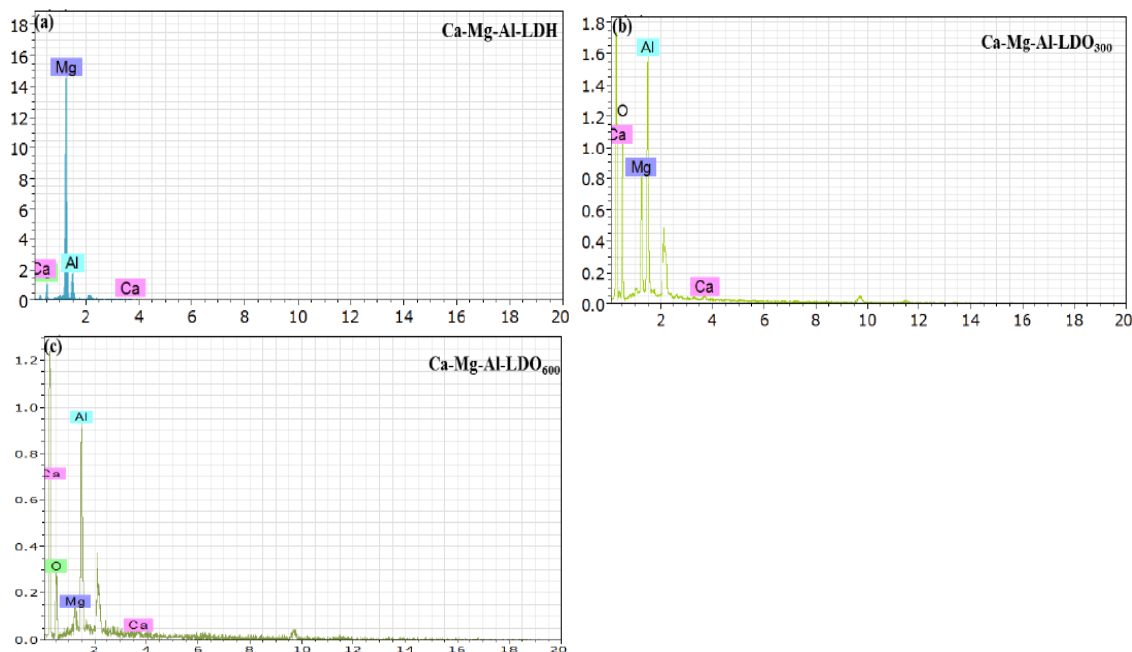


Figure 3: Energy-dispersive spectroscopy (EDS) results of Ca-Mg-Al-LDH(a)&(b), Ca-Mg-Al-LDO300(c) &(d) and Ca-Mg-Al-LDO 600°C

The element mapping test results of the three samples in the experiment are shown as Figure 3. Comparing the results in each image, we can see that Ca, Mg, Al, and O are uniformly distributed in the internal structure. By analyzing the contents of the four elements we can know that, with the continuous increase of the

calcination temperature, the distribution of Ca and Al is more concentrated and has a higher content, and the results obtained by the test are consistent with the results of EDS.

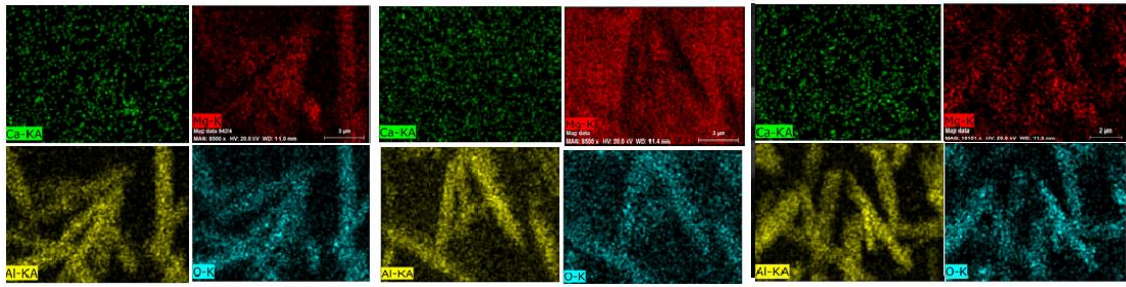


Figure 4: Element mapping of the homogenous dispersion of Ca, Mg, Al and O elements in the as-prepared Ca-Mg-Al-LDH(a)&(b), Ca-Mg-Al-LDO300(c)&(d) and Ca-Mg-Al-LDO 600 (e)

The crystal structure morphologies of Ca-Mg-Al-LDH and Ca-Mg-Al-LDO<sub>x</sub> are determined by XRD of a Cu-K $\alpha$  diffraction source ( $\lambda=1.5418\text{\AA}$ ). Ca-Mg-Al-LDO<sub>x</sub> has a very similar crystal structure morphology. In the Ca-Mg-Al-LDH spectrum, there are very obvious diffraction peaks where  $2\theta=15.22^\circ$ ,  $26.87^\circ$ ,  $30.77^\circ$ ,  $31.93^\circ$ ,  $34.81^\circ$ ,  $42.18^\circ$ ,  $45.30^\circ$  and  $52.67^\circ$ , they respectively belong to the (003), (006), (100), (009), (023), (015), (018), and (1010) crystal faces of Ca-Mg-Al-LDH, indicating that Ca-Mg-Al-LDH has a hydrotalcite-like structure with higher crystallinity and purity. The value of  $d$  and the microcrystalline size can be calculated by combining Bragg's formula, the calculation results are shown as Table 2. The results show that the basic structure and crystalline phase transition of Ca-Mg-Al-LDH and Ca-Mg-Al-LDO<sub>x</sub> change greatly with the increasing of calcination temperature.

Table 2: Crystallite sizes and  $d$ -spacing of Ca-Mg-Al-LDH and Ca-Mg-Al-LDO<sub>x</sub> from XRD analysis

sample	d-spacing(A)		Microcrystalline size (nm)			
	100	9	15	100	9	15
Ca-Mg-Al-LDH	2.92	2.82	2.15	24.3	17.6	18.7
Ca-Mg-Al-LDO (200)	2.91	2.8	2.14	24.4	19.2	15.4
Ca-Mg-Al-LDO (300)	2.92	2.8	2.13	22.8	20.8	18.1
Ca-Mg-Al-LDO (400)	2.91	2.8	2.13	15.6	24.1	20.2
Ca-Mg-Al-LDO (500)	3.01	2.91	2.12	21.6	14.6	12.3
Ca-Mg-Al-LDO (600)	3.03	2.9	2.12	20.5	21.1	16.2

### 3.2 Research on dynamic behavior

In order to study the adsorption rate (such as mass transfer or chemical reaction) of the adsorption process, the influence of contact time on the U(VI) adsorption of Ca-Mg-Al-LDH, Ca-Mg-Al-LDO300 and Ca-Mg-Al-LDO600 is within the first 2 hours, the removal efficiency of U(VI) adsorbed by Ca-Mg-Al-LDO300 and Ca-Mg-Al-LDO600 increased rapidly, especially in the first 10 minutes, the removal rate could exceed 50%. However, the adsorption rate and adsorption capacity of U(VI) by Ca-Mg-Al-LDH increase very slowly, mainly because Ca-Mg-Al-LDH has a smoother surface and fewer material defects.

This adsorption process can be simulated by the quasi-first-order kinetic and quasi-second-order kinetic model. The basic calculation formulas are as follows:

$$\ln(q_e - q_t) = \ln q_e - k_1 t \quad (5)$$

$$\frac{t}{q_t} = \frac{1}{k_2 q_e^2} + \frac{t}{q_e} \quad (6)$$

In the above formulas,  $q_t(\text{mg}\cdot\text{g}^{-1})$  and  $q_e(\text{mg}\cdot\text{g}^{-1})$  respectively represent the adsorption capacity values at equilibrium,  $k_1(\text{min}^{-1})$  and  $k_2(\text{g}\cdot\text{mg}^{-1}\cdot\text{min}^{-1})$  represent quasi-first-order and quasi-second-order kinetic constant values. The above two sets of parameter values are obtained by calculating the linear graphs of  $\ln(q_e - q_t)$  vs  $t$  or  $t/q_t$  vs  $t$ , respectively, see Table 3 for related parameters. The analysis proves that this adsorption

process is more consistent with the analysis results of the quasi-second-order kinetic model, and it can be proved that the adsorption of U(VI) can be attributed to the category of chemical adsorption process.

Table 3: Kinetic parameters for U(VI) adsorption by Ca-Mg-Al-LDH, Ca-Mg-Al-LDO 300 and Ca-Mg-Al-LDO600

Adsorbents	Quasi first order model		Quasi second order model		
	q1, cal (mg.g <sup>-1</sup> )	kf(min <sup>-1</sup> ) R2	q2,cal(mg.g <sup>-1</sup> )	Ks (g.mg <sup>-1</sup> .min <sup>-1</sup> )	R2
Ca-Mg-Al-LDH	103.4	0.131	0.988	145.6	0.986
Ca-Mg-Al-LDO300	74.4	0.087	0.738	226.2	0.998
Ca-Mg-Al-LDO600	53.8	0.132	0.734	249.4	0.999

### 3.3 Adsorption mechanism and environmental application strategy

The repairing effect of natural clay minerals is of great significance to environmental protection and can avoid second-time pollution to the environment. The method of changing the calcination temperature to realize the synthesis process of the hydrotalcite material and the tunable performance for U(VI) adsorption is very useful for solving the environmental pollution problem. The specific steps are shown in the schematic diagram in Figure 7.

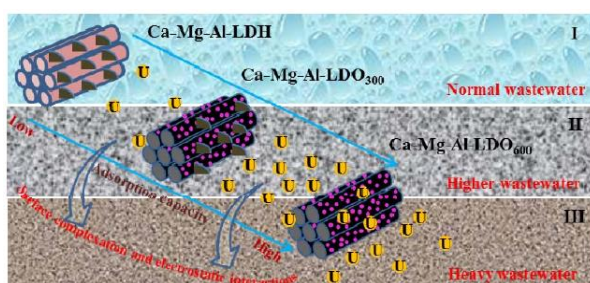


Figure 7: Schematic representation mechanism and environmental behavior of U(VI) adsorption by Ca-Mg-Al-LDH and Ca-Mg-Al-LDOx

The basic mechanism of the adsorption of U(VI) by Ca-Mg-Al-LDH and Ca-Mg-Al-LDOx is mainly the super-strong surface complexation and electrostatic interaction, with the gradual increase of the calcination temperature, the defects on the surface of the material are continuously increased and the active sites are fully exposed, all of which can promote the smooth progress of the adsorption process. Research results can be targeted at different types and different levels of various environmentally harmful pollutants, through a controlled, layered and adjustable adsorbent, we can perform efficient treatment, achieving ultimate rational recycling and reuse of pollutants, which is of great significance for environmental purification and in-situ remediation.

## 4. Conclusion

This paper takes the hydrotalcite materials' few oxygen-containing functional groups and low adsorption capacity as the main research contents for in-depth studies, two main conclusions are obtained as follows:

(1) Experiments of the influence of different adsorption conditions show that: the adsorption isotherms of various materials in the experiment can be fitted by Sips model. Studies have shown that the adsorption process at low U(VI) concentration belongs to polymolecular layer adsorption, but the adsorption process at high U(VI) concentration belongs to monomolecular layer adsorption.

(2) In the experimental study of adsorption mechanism, it can be found that the uranyl maintains the U(VI) elemental valence during the adsorption process, and no electric valence conversion occurs. The remaining chemical materials Ca-Mg-Al-LDH and Ca-Mg-Al-LDOx mainly achieve the separation and enrichment of U(VI) through surface complexation and electrostatic interactions. The research results can achieve the ultimate rational recycling and reuse of pollutants, which is of great significance for the prevention and control of environmental pollution.

## References

- Anirudhan T.S., Jalajamony S., 2013, Ethyl thiosemicarbazide intercalated organophilic calcined hydrotalcite as a potential sorbent for the removal of uranium(vi) and thorium(iv) ions from aqueous solutions. *Journal of Environmental Sciences*, 25(4), 717-725, DOI: 10.1002/bit.260240415.
- Anirudhan T.S., Jalajamony S., 2013, Ethyl thiosemicarbazide intercalated organophilic calcined hydrotalcite as a potential sorbent for the removal of uranium(VI) and thorium(IV) ions from aqueous solutions. *Journal of Environmental Science (English Edition)*, 25(4), 717-725, DOI: 10.1016/s1001-0742(12)60064-3.
- Bonhoure I, Scheidegger A.M., Wieland E., Dähn R., 2002, Iodine species uptake by cement and csh studied by I k-edge x-ray absorption spectroscopy. *Radiochimica Acta*, 90(9-11/2002), 647-651, DOI: 10.1524/ract.2002.90.9-11\_2002.647.
- Cheng W., Wan T., Wang X., Wu W., Hu B. 2018, Plasma-grafted polyamine/hydrotalcite as high efficient adsorbents for retention of uranium (vi) from aqueous solutions. *Chemical Engineering Journal*, 342, DOI: 10.1016/j.cej.2018.01.100.
- Durán-Blanco J.M., López-Muñoz B.E., Olguín M.T., 2013m Influence of ph on u(vi) adsorption using a thermally-treated mg-al hydrotalcite and a natural zeolite in a batch system. *Separation Science & Technology*, 48(5), 797-804, DOI: 10.1080/01496395.2012.707727.
- Hennig B.C, Reich T., Dähn R., Scheidegger A.M., 2002, Structure of uranium sorption complexes at montmorillonite edge sites. *Radiochimica Acta*, 90(9-11/2002), 653-657, DOI: 10.1524/ract.2002.90.9-11\_2002.653.
- Li Y., Wang J., Li Z., Liu Q., Liu J., Liu L., 2013, Ultrasound assisted synthesis of ca-al hydrotalcite for u (vi) and cr (vi) adsorption. *Chemical Engineering Journal*, 218(3), 295-302, DOI: 10.1016/j.cej.2012.12.051.
- Molera M., Eriksen T., 2002, Diffusion of  $^{22}\text{Na}^+$ ,  $^{85}\text{Sr}^{2+}$ ,  $^{134}\text{Cs}^+$  and  $^{57}\text{Co}^{2+}$  in bentonite clay compacted to different densities: experiments and modeling. *Radiochimica Acta*, 90(9-11/2002), 753-760, DOI: 10.1524/ract.2002.90.9-11\_2002.753.
- Nakata K., Nagasaki S., Tanaka S., Sakamoto S., Tanaka Y., Ogawa T., 2002, Sorption and reduction of neptunium(v) on the surface of iron oxides. *Radiochimica Acta*, 90(9-11/2002), 665-669, DOI: 10.1524/ract.2002.90.9-11\_2002.665.
- Suc N.V., 2012, Adsorption of u(vi) from aqueous solution onto hydrotalcite-like compounds, 9(2), 669-679, DOI: 10.1155/2012/182585.